

UCSF

UC San Francisco Previously Published Works

Title

The role of macrophages in right ventricular remodeling in experimental pulmonary hypertension

Permalink

<https://escholarship.org/uc/item/7qg2511m>

Journal

Pulmonary Circulation, 12(3)

ISSN

2045-8932

Authors

Gu, Sue
Mickael, Claudia
Kumar, Rahul
et al.

Publication Date





2022-07-01

DOI

10.1002/pul2.12105

Peer reviewed

The role of macrophages in right ventricular remodeling in experimental pulmonary hypertension

Sue Gu^{1,2}  | Claudia Mickael^{1,3} | Rahul Kumar⁴ | Michael H. Lee⁴  |
Linda Sanders^{1,3} | Biruk Kassa⁴ | Julie Harral² | Jason Williams⁵  |
Kirk C. Hansen⁵ | Kurt R. Stenmark² | Rubin M. Tuder^{1,3} | Brian B. Graham⁴ 

¹Department of Medicine, Division of Pulmonary Sciences and Critical Care Medicine, University of Colorado Anschutz Medical Campus, Aurora, Colorado, USA

²Cardiovascular Pulmonary Research Lab, University of Colorado School of Medicine, Aurora, Colorado, USA

³Department of Medicine, Program in Translational Lung Research, University of Colorado Anschutz Medical Campus, Aurora, Colorado, USA

⁴Department of Medicine, Division of Pulmonary and Critical Care Medicine, Zuckerberg San Francisco General Hospital and Trauma Center, University of California, San Francisco, California, USA

⁵Biochemistry and Molecular Genetics, University of Colorado Anschutz Medical Campus, Aurora, Colorado, USA

Correspondence

Sue Gu, Department of Medicine, University of Colorado Anschutz Medical Center, Research Complex II, Division of Pulmonary Sciences and Critical Care Medicine, 12700 East 19th Ave 9C03, Aurora, CO 80045, USA.
Email: sue.gu@cuanschutz.edu

Brian B. Graham, Department of Medicine, Division of Pulmonary and Critical Care Medicine, Zuckerberg San Francisco General Hospital and Trauma Center, University of California San Francisco, 1001 Potrero Ave, Bldg 5, Room 5J1, San Francisco, CA, 94127, USA.
Email: brian.graham@ucsf.edu

Funding information

National Institutes of Health, Grant/Award Numbers: 5T32HL007085, 5T32HL007171, F32HL151076, P01HL152961, R01HL135872, R25HL14166; Actelion Pharmaceuticals, Grant/Award Number: Entelligence Award 2020; American Heart Association, Grant/Award Number: 19CDA34730030; American Thoracic Society, Grant/Award Number: ATS Foundation Pulmonary Hypertension Association

Abstract

Right ventricular (RV) failure is the primary cause of death in pulmonary hypertension (PH), but the mechanisms of RV failure are not well understood. We hypothesized macrophages in the RV contribute to the RV response in PH. We induced PH in mice with hypoxia (FiO₂ 10%) and *Schistosoma mansoni* exposure, and in rats with SU5416-hypoxia. We quantified cardiac macrophages in mice using flow cytometry. Parabiosis between congenic CD45.1/.2 mice or Cx3cr1-green fluorescent protein and wild-type mice was used to quantify circulation-derived macrophages in experimental PH conditions. We administered clodronate liposomes to Sugen hypoxia (SU-Hx) exposed rats to deplete macrophages and evaluated the effect on the extracellular matrix (ECM) and capillary network in the RV. In hypoxia exposed mice, the overall number of macrophages did not significantly change but two macrophage subpopulations increased. Parabiosis identified populations of RV macrophages that at steady state is derived from the circulation, with one subpopulation that significantly increased with PH stimuli. Clodronate treatment of SU-Hx rats resulted in a change in the RV ECM, without altering the RV vasculature, and correlated with improved RV function. Populations of RV macrophages increase and contribute to RV remodeling in PH, including through regulation of the RV ECM.

KEYWORDS

adaptation, hypoxia, inflammation, right heart, *Schistosoma*

This is an open access article under the terms of the Creative Commons Attribution-NonCommercial License, which permits use, distribution and reproduction in any medium, provided the original work is properly cited and is not used for commercial purposes.

© 2022 The Authors. *Pulmonary Circulation* published by John Wiley & Sons Ltd on behalf of Pulmonary Vascular Research Institute.

INTRODUCTION

Pulmonary arterial hypertension (PAH) is a rare condition characterized by remodeling of the small pulmonary arteries resulting in a progressive increase in pulmonary vascular resistance and right ventricular (RV) failure. Despite advances in therapies over the past few decades, the median survival remains only 7–9 years after the time of diagnosis.¹ RV function is the most important predictor of morbidity and mortality in all forms of pulmonary hypertension (PH),^{2,3} yet there are no specific therapies available that address RV function.

The RV adaptive response to chronic PH includes hypertrophy, fibrosis, inflammation, and capillary rarefaction.⁴ Our prior work has demonstrated that capillary rarefaction is driven by RV hypertrophy outpacing compensatory angiogenesis, rather than by endothelial cell death or capillary dropout.⁵ However, drivers of the cellular responses to pressure overload are unknown. We propose that RV macrophages play a central role in the adaptation that the RV undergoes in chronic PH, and may present a novel therapeutic target to improve outcomes for patients with PH.

Macrophages are a heterogeneous population of immune cells that fulfill myriad tissue-specific and niche-specific functions in homeostasis and inflammation, and are the major immune cells in the heart under steady state conditions.⁶ Studies using fate mapping, parabiosis, and transplantation have identified distinct subsets of cardiac macrophages with differing origins which determine cell programming and behavior.^{7–10} Long-lived tissue-resident cardiac macrophages are derived from yolk sac progenitors during embryonic development and are replenished primarily through local proliferation, serving physiologic and homeostatic functions including coronary development, cardiomyocyte proliferation and physiologic hypertrophy.⁸ In response to cardiac stress such as ischemia or pressure overload, bone marrow derived monocytes are recruited to the heart where they mature into macrophages that participate in the initiation of inflammation, ventricular remodeling and scar formation as well as a wide range of interactions that alter the extracellular matrix (ECM).^{8,11–13} There is also evidence that in cancer and wound repair, macrophages support angiogenesis by secreting proangiogenic growth factors and matrix-remodeling proteases, and also by physically interacting with the sprouting vasculature to assist the formation of complex vascular networks.^{14,15} RV macrophages have previously not been quantified or characterized in response to experimental PH.

Here we aim to quantify and characterize the RV macrophage response in experimental PH by surface markers. We hypothesized that monocyte-derived macrophages are recruited into the right ventricle in PH, and that these cells functionally promote RV remodeling including regulation of the ECM and compensatory angiogenesis.

METHODS

Animal models

All animal experiments were approved by the University of Colorado Institutional Animal Care and Use Committee. CD45.1 (B6.SJL-*Ptprca^aPepc^b*/Boy) and CD45.2 (C57BL/6) mice were purchased from Jackson Laboratory and Charles River Laboratories. Cx3cr1-green fluorescent protein (GFP) mice were purchased from Jackson Laboratory and bred in-house. Mice were used at 6–10 weeks of age and housed in a specific pathogen-free environment.

Mouse hypoxia PH model

We exposed male and female C57BL/6 mice (Jackson Laboratory) at 6 weeks of age to 10% FiO₂ at Denver altitude for 24 h, 48 h, or 7 days duration followed by terminal RV harvest. The partial pressure of oxygen was regulated by a ProOx 110 (Biospherix) oxygen sensor and feedback loop regulating the flow of nitrogen gas into the chamber.

Mouse schistosomiasis PH model

We have previously published studies using an experimental schistosomiasis-induced PH model,¹⁶ which models the natural history of the parasite infection, notably in relation to the pulmonary vascular disease. Mice were sensitized with 240 purified *S. mansoni* eggs/gram body weight (purified from the livers of infected Swiss-Webster mice; provided by the Biomedical Research Institute) injected intraperitoneally (IP), followed 2 weeks later by challenge with 175 *S. mansoni* eggs/gram body weight injected by tail vein. We have previously shown that mice that receive intravenous (IV) *S. mansoni* egg injection develop PH, while those that receive only IP *S. mansoni* egg injection do not.¹⁶ One week later, the mice underwent terminal right heart catheterization and tissue collection.

Rat Sugen hypoxia (SU-Hx) PH model

The Sugen (SU5416) hypoxia model (SU-Hx) is a well-established model of PH in which exposure to Sugen, a selective small molecule inhibitor of VEGF receptor tyrosine kinase activity, along with hypoxia results in angio-ablative lesions in the pulmonary vasculature resembling group I PAH in humans, resulting in severe PH and RV failure.¹⁷ Female Sprague-Dawley rats (Taconic Biosciences) at 6–8 weeks of age received subcutaneous SU5416 (Tocris Bioscience) 20 mg/kg dissolved in carboxymethylcellulose and then diluted in 1:1 with phosphate buffered saline (PBS) just before being placed into hypobaric hypoxia at simulated elevation 18,000 ft. After 21 days, the rats underwent terminal RV catheterization for pressure–volume measurements followed by RV tissue collection. The rat RV tissue was placed into water to determine the absolute volume of the tissue (Archimedes' principle), and then divided into eight pieces and numbered. An 8-sided die was cast to randomly determine which tissue pieces would be snap frozen or placed in formalin.

Clodronate treatment

One day before SU-Hx treatment, rats received 50 mg/kg clodronate liposomes, divided into 500 μ l intravascular (IV) injection via tail vein, with the remaining volume delivered IP. Control rats received the equivalent volume of PBS liposomes via tail vein and IP. On Days 7 and 14, the rats received additional 25mg/kg clodronate liposome or PBS liposome injections. On Day 21, the rats underwent RV catheterization.

Parabiosis

Pairs of female CD45.1 (B6.SJL-*Ptprc*^a*Pepc*^b/Boy) and CD45.2 (C57BL/6) mice, or Cx3cr1-GFP and wild-type C57BL/6 mice were surgically joined using a published protocol to create a shared circulatory system.¹⁸ Male mice were not used in parabiosis experiments due to our previous experience with high rates of fighting resulting in wound dehiscence and death. Briefly, mice were continuously anesthetized with isoflurane and kept on a heated pad throughout surgery. Animal partners were shaved on opposing sides followed by an incision from the elbow to the knee. First, joints of the elbows and knees were sutured together using 3–0 nonabsorbable sutures. Then, dorsal–dorsal and ventral–ventral skin was joined using an absorbable 5–0 Vicryl suture.

Finally, mice were administered carprofen for pain relief, as needed, and were kept on antibiotic Septra diet to prevent postoperative infections. The mouse pairs underwent 2 weeks of recovery before any further experimentation.

Rat pressure–volume measurements

Rats were anesthetized with isoflurane. A tracheal cannula was inserted and connected to a Hallowell EMC Anesthesia Workstation and anesthesia was maintained at 1.5%–2.5% isoflurane in 21% oxygen/balance nitrogen. A pressure-only catheter (FTH-1611B-0018; Transonic/Scisense) was placed into the femoral artery for continuous recording of systemic pressure. The RV, pulmonary artery (PA), and left ventricular (LV) pressures were directly measured with a 1.9-Fr pressure–volume catheter (Transonic/Scisense; FTH-1912B-6018) inserted into the heart directly through the wall via a diaphragmatic approach. The pericardium was resected and a small entry hole was made at the base of the RV with a 26-gauge needle. The pressure–volume catheter was inserted and advanced along the length of the RV. Steady-state hemodynamics were collected with short pauses in ventilation to eliminate ventilator artifact from the pressure–volume recordings. Occlusions of the inferior vena cava were also performed to decrease preload and obtain an accurate end-systolic pressure–volume relationship. The catheter was then placed into the PA and pressure measurements were recorded. One final puncture was made in the apex of the LV and the catheter was placed along the length of the LV for measurement of steady-state data in the LV. Data were recorded continuously with LabScribe 2 (iWorx) and analyzed offline.

Immunostaining and flow cytometry

Immunostaining of rat RV tissue was performed using the reagents in Supporting Information: Table 1. For rat RV macrophage quantification, five images from each RV were taken at 20 magnification. Quantification was done with STEPanizer stereology tool (www.stepanizer.com) by an experimenter blind to the treatment conditions.¹⁹ Flow cytometry was performed on digested RV tissue from mice using the reagents in Supporting Information: Table 2 in the Online Supporting Information. IV myeloid cells were labeled by retro-orbital injection of fluorescently conjugated anti-CD45 antibody just before sacrifice.

Vascular stereology

We followed a previously described approach to quantify RV vascular structure by stereology.⁵ In brief, 4–6 images per sample were randomly and uniformly obtained from FITC-Isolectin B4-stained isotropically oriented sections, which were digitally analyzed to identify the tissue area and number of vessel intersections with the sampling plan. The length per unit volume and average radius of tissue served per vessel were then calculated,⁷ including a correction factor of 20% for shrinkage of cardiac tissue due to processing.⁵

Matrisome protein analysis

Materials and methods for matrisome analysis are described in detail in the Online Supporting Information. Briefly, the sample was powderized in liquid nitrogen using a ceramic mortar and pestle, homogenized, and vortexed three times to obtain three fractions of supernatant which were combined to make the cell fraction, with the remaining sample spun and divided into soluble ECM and insoluble ECM fractions. Samples were subsequently digested with trypsin and analyzed by nano-UHPLC-MS/MS (Easy-nLC1000; QExactive HF; Thermo Fisher Scientific). Instrument raw spectrum files were directly loaded into Proteome Discoverer 2.2 and were searched in mascot against the Uniprot Rat database using Mascot (v2.3.1), and a common contaminants database. Significant proteins were uploaded into Ingenuity Pathway Analysis (Qiagen) to explore significantly enriched networks and canonical pathways.

Statistics

t-test and analysis of variance (ANOVA) with post hoc Tukey test were performed for normally distributed data, and rank-sum test and ANOVA on ranks with post hoc Dunn's test for non-normally distributed data using the software GraphPad Prism, MetaboAnalyst, and SigmaPlot 13.0. $p < 0.05$ was considered statistically significant.

RESULTS

Two RV cardiac macrophage subpopulations are increased by acute hypoxia

To identify and quantify RV macrophages after hypoxia exposure, flow cytometry analysis was performed on a

digest of cells isolated from the mouse RV. Previous work has demonstrated that the coexpression of markers MerTK and CD64 is highly specific for macrophages.²⁰ We excluded IV myeloid cells labeled by intravenously injected fluorescently conjugated anti-CD45 antibody just before sacrifice. We identified interstitial macrophages with further gating for CD45⁺, CD11b⁺, MerTK⁺, and CD64⁺ cells (Figure 1A). MerTK⁺CD64⁺ macrophages were further analyzed using CD11c and MHCII to identify three subpopulations which have been previously shown to be present in the lungs, heart and liver²¹ based on their expression levels of CD11c and MHCII: CD11c^{lo}MHCII^{lo} (IM1); CD11c^{lo}MHCII^{hi} (IM2); and CD11c^{hi}MHCII^{hi} (IM3). IV monocytes were identified based on gating for IV-CD45⁺, Ly6C⁺, and CD11b⁺ cells.

We observed no significant change in the overall number of extravascular RV macrophages across all timepoints (Figure 1B). When analyzing subgroups of macrophages, we observed that the number of IM1 and IM3 macrophages was significantly increased after 48 h and 7 days of hypoxia compared to normoxic conditions, with no change in the IM2 population (Figure 1C). Compared to normoxia, the absolute number of IV monocytes was also significantly increased after 48h and 7 days of hypoxia (Figure 1D).

Assessment of RV macrophage recruitment from the circulation

To determine if the RV macrophages were derived from the circulation or expansion of prepositioned interstitial cells, we performed parabiosis experiments. We surgically conjoined C57BL/6 (wild-type) and Cx3cr1-GFP mice, which label monocytes and macrophages with GFP. After allowing for 2 weeks of recovery and development of shared circulation, two pairs of C57BL/6 + Cx3cr1-GFP mice were placed into a FiO₂ 10% hypoxia chamber for 48 h while two pairs remained in normoxia (Figure 2A). One normoxic pair experienced wound dehiscence and did not survive to the time of harvest. After RV macrophages were identified by flow cytometry, they were further dichotomized based on GFP fluorescence as originating from self or from the partner mouse (Figure 2A). We observed in the parabiosis pairs that <10% of RV macrophages in acute hypoxia were derived from the partner parabiont, while in the normoxic pair there was significant variation in the percentage of RV macrophages derived from the partner parabiont (3% and 58%) (Figure 2B).

To follow-up these results, we surgically joined CD45.1 and CD45.2 congenic mice ($N = 3$ pairs). Two weeks after surgery each parabiont received IP injections

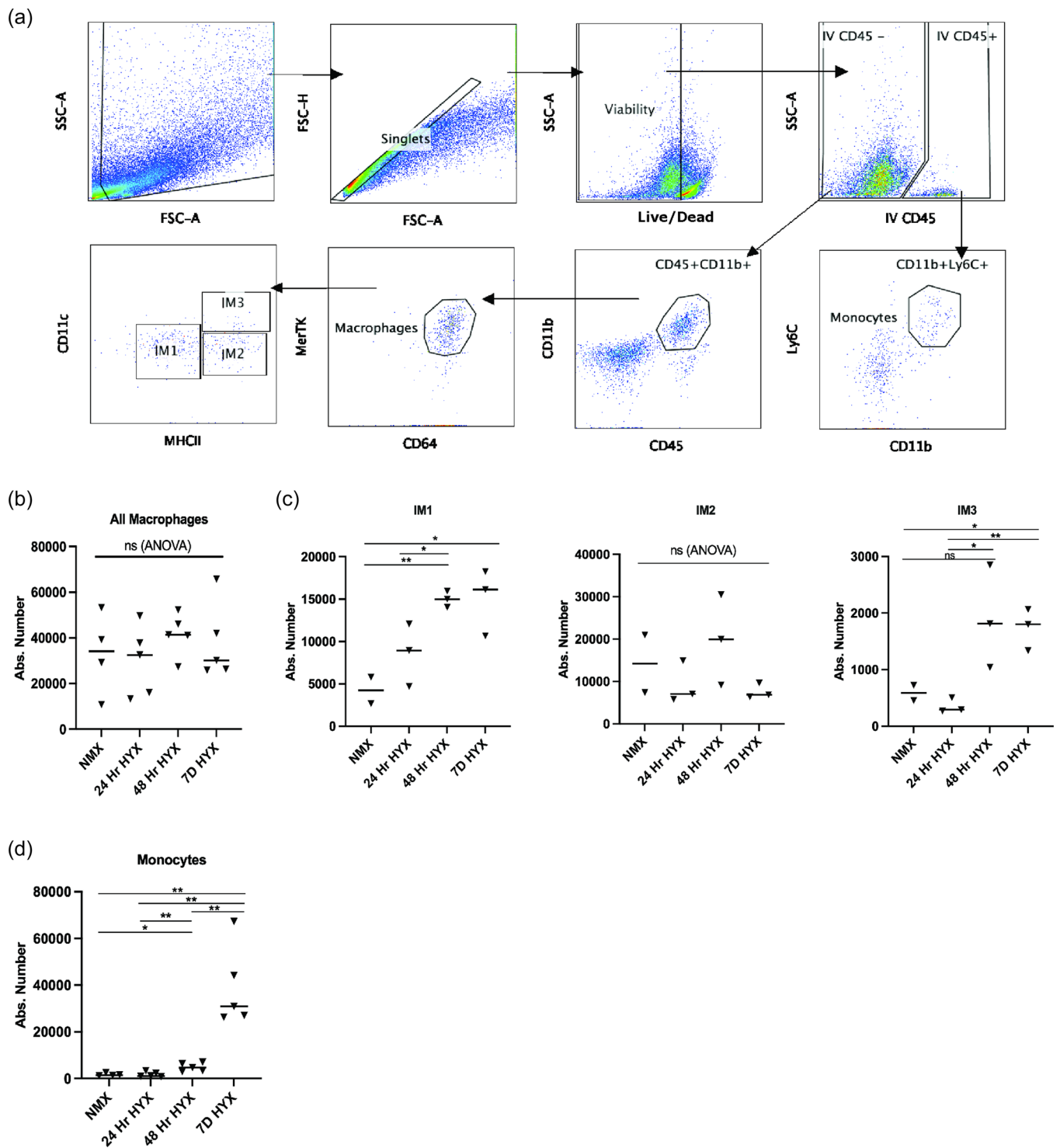
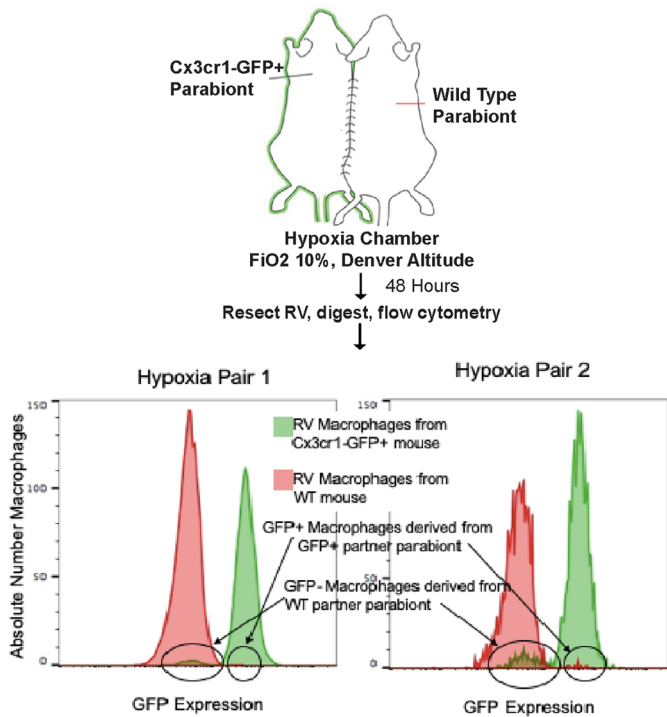
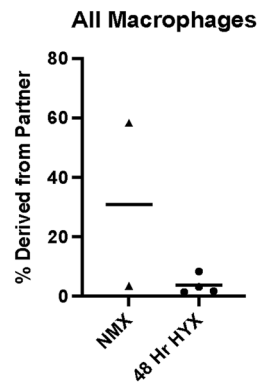


FIGURE 1 Murine right ventricular (RV) interstitial macrophage and intravascular (IV) monocyte identification and quantification in hypoxia (a). Representative flow cytometry gating strategy. After excluding debris and doublets using forward (FSC) and side scatter (SSC), cells were further gated for viable cells. Fluorescently conjugated CD45 (IV-CD45) antibody injected retro-orbitally before sacrifice was used to separate IV from interstitial myeloid cells. IV-CD45 positive cells were further gated on CD11b and Ly6C to identify circulating monocytes. IV-CD45 negative interstitial cells were further gated on myeloid markers CD45 and CD11b, and E macrophage specific markers CD64 and MerTK. Macrophages were divided by expression of CD11c and MHCII into IM1 (CD11c^{lo}MHCII^{lo}), IM2 (CD11c^{lo}MHCII^{hi}) and IM3 (CD11c^{hi}MHCII^{hi}) subsets (b). Quantification of all IV-CD45 negative, CD45 + CD11b + CD64 + MerTK+ RV interstitial macrophages in normoxia (NMX) and hypoxia (HYX) at 24 h, 48 h, and 7 days ($n = 4, 5, 5, 5$), (analysis of variance [ANOVA] shown, ns) (c). Quantification of 3 RV macrophage subpopulations in normoxia (NMX) and hypoxia (HYX) at 24h, 48 h, and 7 days ($n = 2, 3, 3, 3$) (ANOVA and post hoc Tukey test shown, * $p < 0.05$, ** $p < 0.01$, ns) (d). Quantification of IV monocytes ($n = 4, 5, 5, 5$ per group), (ANOVA and post hoc Tukey test shown; * $p < 0.05$; ** $p < 0.01$). ns, nonsignificant.

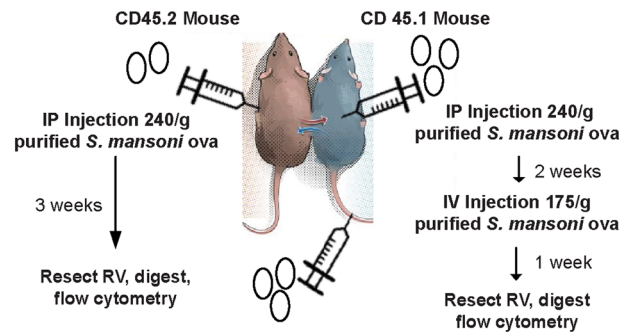
(a) Hypoxia Parabiosis Experimental Design



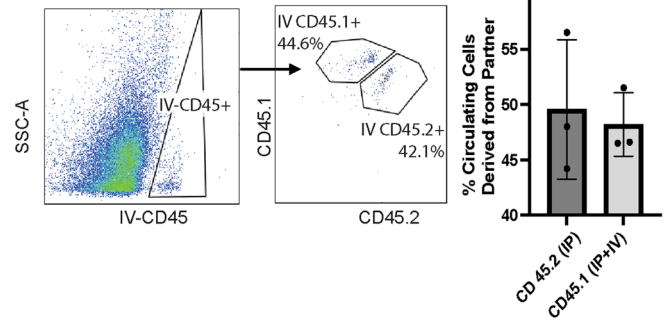
(b) Partner Derived RV Macrophages in Hypoxia PH



(c) Schistosoma-PH Parabiosis Experimental Design



(d) Determination of Origin of Circulating Myeloid Cells in Schistosoma-PH Parabiosis



(e) Partner Derived RV Macrophages in Schistosoma-PH

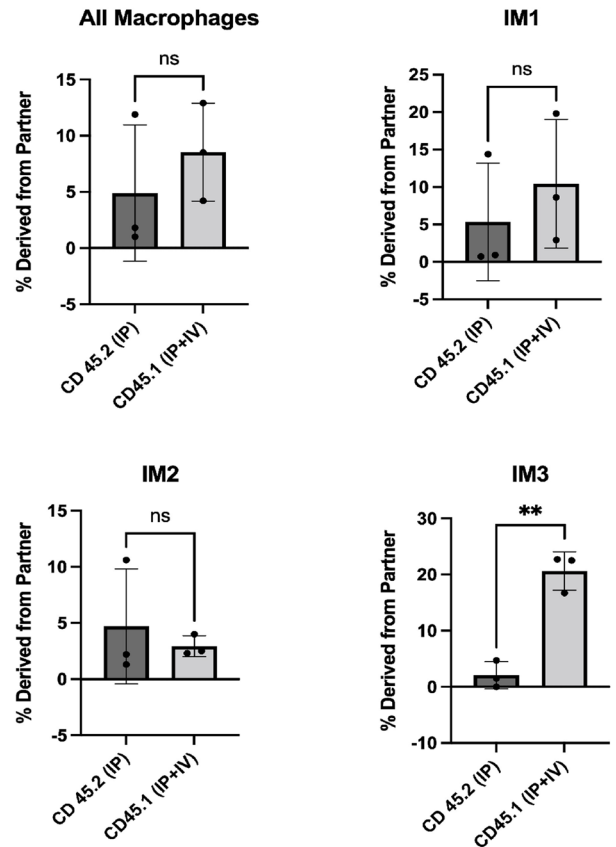


FIGURE 2 (See caption on next page)

of *S. mansoni* eggs (Figure 2C). Two weeks after the IP injection, only the CD45.1 mouse in each pair received an additional IV injection of *S. mansoni* eggs to induce PH in that mouse specifically.²² One week later, all pairs of mice underwent terminal RV harvest. Single cell suspensions were prepared and analyzed with flow cytometry. Using the IV-CD45 and CD45.1/2 markers, we confirmed successful chimerism of the circulation with a mean of 46% and 44% of circulating myeloid cells derived from the partner mouse (Figure 2D). We observed a mean of 8.5% partner-derived overall RV macrophages in the IV egg-challenged PH mice, which was not significantly different than a mean of 4.9% of overall RV macrophages that were partner-derived in the non-PH mice that received *S. mansoni* eggs IP only (Figure 2E). When we analyzed subgroups of macrophages, we observed that the percentage of partner derived IM3s (CD11c^{hi}MHCII^{hi}) was significantly increased in the *Schistosoma*-PH challenged mice (20.6% vs. 2%, $p = 0.0015$), whereas the percentage of IM1 (CD11c^{lo}MHCII^{lo}) macrophages derived from the partner mouse was modestly increased but not statistically different (10.4% vs. 5.4%, $p = 0.5$) (Figure 2E).

These experiments suggest that a small proportion of RV macrophages are derived from the circulation in steady state, and PH stimuli significantly recruits at least one macrophage subpopulation from the circulation into the RV interstitium.

Clodronate treatment improves RV function

To determine a functional role for macrophages in RV adaptation in PH, we used previously established monocyte/macrophage depletion approaches with clodronate liposomes in rat SU-Hx.^{8,23–27} We have previously shown

that macrophage depletion with clodronate starting before hypoxia exposure decreases pulmonary interstitial macrophages and partially decreases but does not abrogate the PH phenotype.²³

After exposure to SU5416 and 3 weeks hypoxia (SU-Hx), and clodronate administration on Days 0, 7, and 14 (timeline shown in Figure 3A), rats underwent RV catheterization on Day 21. Immunostaining of harvested rat RV tissue with the macrophage marker F4/80 showed a trend towards decreased RV macrophages in clodronate-treated rats (Figure 3B). RV catheterization data revealed severely elevated RV systolic pressure in both the PBS liposome and clodronate treated rats, with no significant difference between groups in RV afterload measured by arterial elastance (Ea), or in RV hypertrophy measured by Fulton Index (Figure 3C). Multibeat pressure–volume loop analysis showed a significant improvement in RV contractility and systolic function measured by end-systolic elastance (Ees) and maximal elastance (Emax), as well as improved RV/PA coupling measured by the ratio of Ees to Ea (Ees/Ea ratio) and by the Emax/Ea ratio (Figure 3C; full rat RV hemodynamics data in Supporting Information: Table 3).

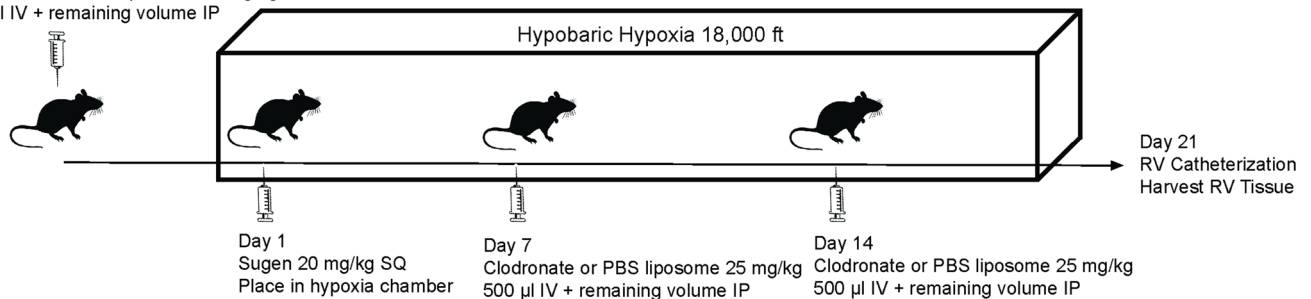
The RV ECM in PH is affected by clodronate treatment

The ECM and matricellular composition of RV tissue specimens from the rats were characterized using tissue-compartment resolved proteomics ($n = 6$ clodronate liposome-treated rats, $n = 6$ PBS liposome-treated rats). Principal component analysis revealed a clear separation of the ECM proteins isolated from clodronate-treated rats compared to PBS-treated rats (Figure 4A). Specific differences in the clodronate-treated rats included reductions in multiple ECM component and glycoproteins

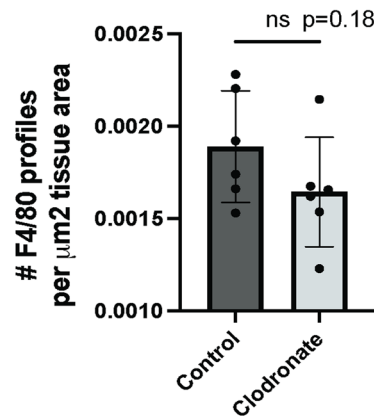
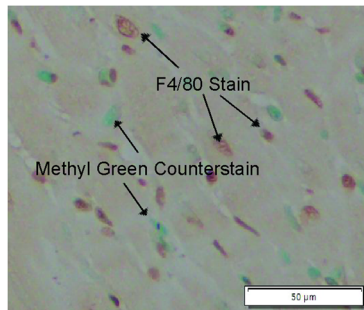
FIGURE 2 Identification of circulation derived right ventricular (RV) macrophages in experimental PH with parabiosis (a). Cx3cr1-GFP and wild-type mice were paired with parabiosis surgery ($n = 3$ pairs). After 2 weeks to allow for recovery and joining of their circulations, two pairs were placed in FiO₂ 10% hypoxia for 48 h (48 h HYX). One pair was housed in normoxia (NMX). After harvest and digestion of the RV, flow cytometry was done to identify macrophages according to our previous gating strategy and GFP fluorescence was used to differentiate self versus partner derived macrophages (b). Percentage of RV macrophages derived from partner circulation in normoxia (NMX) mice ($n = 1$ pair) and hypoxic mice ($n = 2$ pairs) (c). CD45.2 and CD45.1 mice underwent parabiosis surgery ($n = 3$ pairs) and were allowed to recover and join circulation over 2 weeks. The CD45.2 partner mouse was only sensitized to *Schistosoma mansoni* antigen with intraperitoneal (IP) injection of 240/g purified *S. mansoni* ova while experimental PH was induced in the CD45.1 partner mouse with sensitization of IP injection of 250/g purified *S. mansoni* ova followed by intravenous (IV) injection of 175/g purified *S. mansoni* ova after 2 weeks (d). Before sacrifice, mice were injected retro-orbitally with fluorescently conjugated CD45 antibody to label intravascularly circulating myeloid cells. CD45.1/2 markers were used to quantify degree of chimerism in their joint circulation (e). RV digestion and flow cytometry was performed to identify CD45.1 and CD45.2 surface expressing macrophages to differentiate self and partner derived macrophages. Surface markers CD11c and MHCII were used to further characterize subpopulations of IM1, IM2, and IM3 macrophages. (T-test comparisons depicted of partner circulation derived overall macrophages, IM1, IM2, and IM3, $**p < 0.005$). GFP, green fluorescent protein; PH, pulmonary hypertension.

(a) Clodronate in Rat Sugen Hypoxia Experimental Timeline

Day 0

Clodronate or PBS Liposome 50 mg/kg
500 μ l IV + remaining volume IP

(b) Rat RV Macrophage Quantification



(c) Clodronate Treatment Improves RV Contractility and RV/PA Coupling in Rat SU-Hx

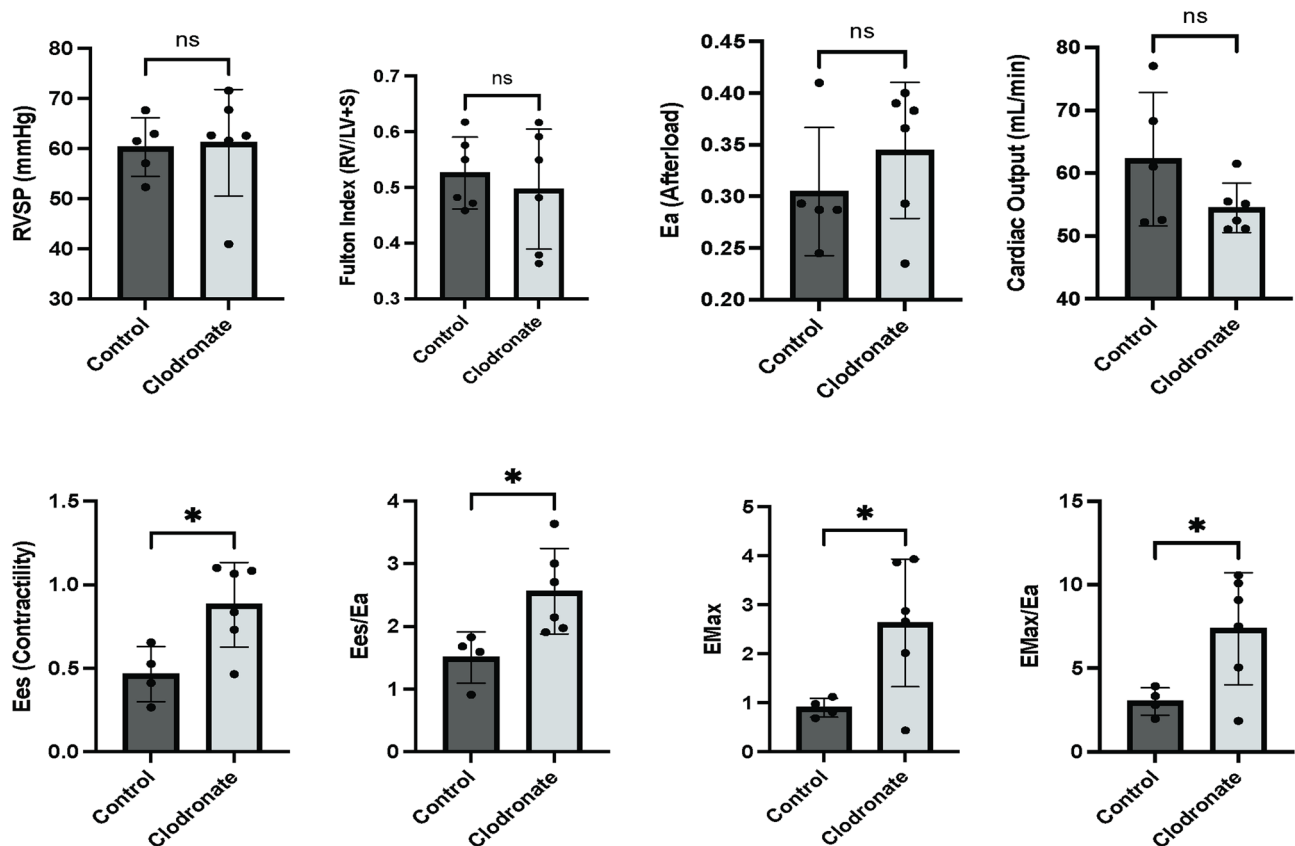


FIGURE 3 (See caption on next page)

including subunits of collagen isoforms I, III, IV and V; fibrillin 1; microfibrillar-associated protein 5; and elastin microfibril interface 1 (Figure 4B).

RV Non-ECM proteins are also affected by clodronate treatment

In addition to these core ECM proteins, we also observed separation of non-ECM proteins in the clodronate treated SU-Hx rats (Figure 5A). Changes identified included reductions in myosin heavy chain 2 (Myh2), dysbindin (Dtnb), cadherin-5 (Cdh5), vimentin (Vim), and titin (Ttn) (Figure 5B). There was also a significant decrease in several proteins involved in mitochondrial function (Ccd51, MTfr11, Pdhx, Agk, Fundc2, and Tomm22). Purine nucleoside phosphorylase (Pnp) and guanine deaminase (Gda), were also significantly decreased. Proteins significantly increased in clodronate treated rats include immunoglobulin kappa constant (Igkc), Protein flightless-1 homolog (Flii), and apolipoprotein E (APOE) (Full set of significant proteins in Supporting Information: Table 4).

We performed pathway analysis on the ECM and non-ECM proteomic data to identify canonical pathways enriched in clodronate treated SU-Hx rats. Pathways that were significantly downregulated included oxidative phosphorylation and GP6 signaling, while pathways that were significantly affected without a clear predicted directionality included mitochondrial dysfunction and sirtuin signaling, a highly conserved pathway important for cardiac homeostasis under physiologic conditions and stress (Supporting Information: Table 5).

Clodronate treatment did not affect RV vascular structure

Randomly oriented pieces of RV tissue from the SU-Hx rats treated with clodronate or PBS control liposomes

were stained with FITC-lectin, and the total RV vascular length and vascular density were quantified using stereology. We observed no significant differences in RV volume of clodronate versus control rats, and quantification with stereology of total RV vascular length showed no significant difference in total RV vessel length, or radius of tissue served per vessel (Figure 6), suggesting that clodronate treatment did not modify RV vessel remodeling in the SU-Hx rat model.

DISCUSSION

Regulators of RV adaptation in PH are not well understood. We identified expansion of RV macrophage subpopulations in the setting of experimental PH challenge including one subset that appears to be derived significantly from the circulation. We then looked for a functional role of RV macrophages, utilizing a well-described method of monocyte/macrophage depletion using clodronate liposomes to see these effects on these features of RV adaptation: vascular and ECM remodeling. Previously we have found that there is significant RV vessel augmentation in rodents with severe PH, but here we found that clodronate treatment did not impact the degree of RV vascular adaptation. However, our RV proteomic analysis of clodronate-treated SU-Hx rats suggested that macrophages regulate RV adaptation through ECM composition and the microenvironment either directly or indirectly such as via interactions with cardiac myocytes or fibroblasts. Clodronate treatment did improve RV function and RV/PA coupling, suggesting that the RV macrophages depleted by clodronate could be promoting RV maladaptation in PH.

The RV ECM is a highly organized, three-dimensional structure that serves important roles including providing the scaffolding for myocytes and other cardiac cells, regulating contractility and relaxation by maintaining ventricular geometry, tissue elasticity and

FIGURE 3 Effect of clodronate treatment on rat right ventricular (RV) adaptation to pulmonary hypertension (a). Experimental timeline of clodronate treatment in rat Sugen hypoxia (SU-Hx) experiment. Female Sprague-Daley rats at 6–8 weeks of age received 50 mg/kg clodronate liposomes, or PBS control liposomes, divided into 500 μ l intravascular (IV) injection via tail vein, with the remaining volume delivered intraperitoneally (IP). Control rats received the equivalent volume of PBS liposomes IV and IP. On Day 1, all rats received subcutaneous (SQ) injection of SQ Sugen (SU5416) 20 mg/kg and were placed into a hypobaric hypoxia chamber at simulated 18,000 ft elevation. On Days 7 and 14, rats received additional 25 mg/kg clodronate liposome or PBS liposome injections IP and IV. On Day 21, rats underwent RV catheterization and RV tissue harvest (b). Quantification of rat RV tissue macrophages with F4/80 immunostaining. RV tissue was stained with F4/80 antibody and methyl green counterstain. F4/80 positive profiles were identified with the STEPanalyzer stereology software and normalized for tissue area. *t*-test shown (c). Rat invasively obtained RV hemodynamics ($n=5$ control, $n=6$ clodronate treated; Grubb's test applied to identify outliers; *t*-test, ns, $*p < 0.05$) and Fulton Index ratio of RV tissue mass to mass of LV plus septum ($n=6$ control, $n=6$ clodronate treated, *t*-test, ns). Ea, arterial elastance; Ees, end-systolic elastance; EMax, maximal elastance; LV, left ventricular; ns, nonsignificant; PA, pulmonary artery; PBS, phosphate buffered saline; RVSP, right ventricular systolic pressure.

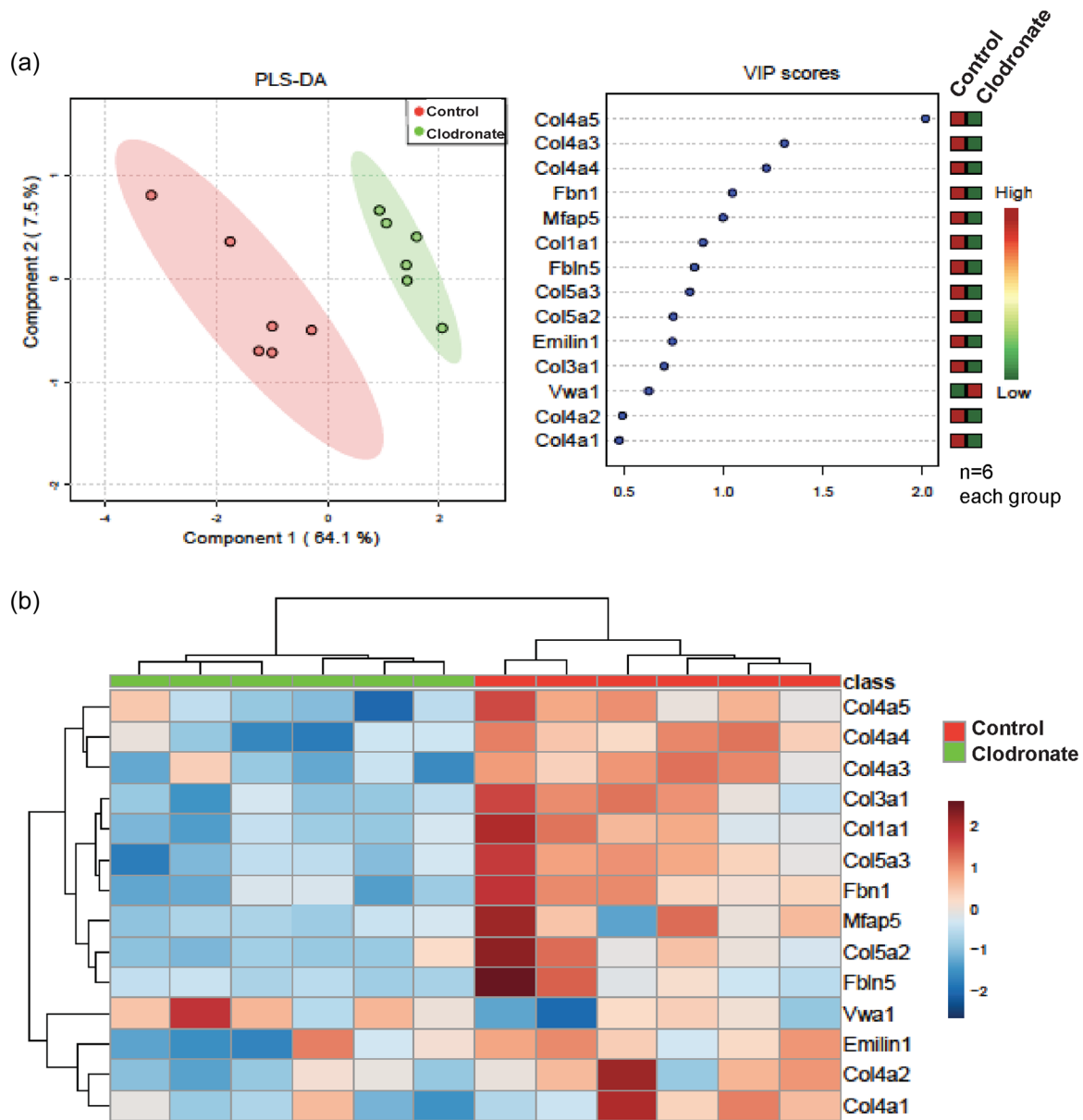


FIGURE 4 Clodronate treatment significantly alters extracellular matrix (ECM) proteins in Rat Sugen hypoxia (SU-HX) (a). Principal component analysis of core ECM proteins in SU-HX rats that received phosphate buffered saline liposomes (control) compared to clodronate liposomes. PLS-DA, partial least squares-discriminant analysis; VIP Score, variable importance projection (b). Heat map with expression of core ECM proteins in control compared to clodronate treated SU-HX rats with differentially expressed proteins with $p < 0.05$.

stiffness, and mediating cell interactions, proliferation, and migration.^{24,28} The RV basement membrane (BM) is a specialized layer of well-organized ECM proteins between cardiac myocytes and the cardiac interstitium, anchoring cells and allowing for cell alignment, cell-to-cell signaling and electrical communication.²⁸ Collagen type IV is the most abundant protein in the BM and forms the scaffold upon which other BM components adhere. Deficiency of Col4a1/Col4a2 (collagen type IV a1 chain/collagen type IV a2 chain) in mice is embryonically lethal due to BM structural instability as the developing heart is subjected to increasing mechanical

stress.²⁹ In rat hypoxia-PH induced RV hypertrophy, increased collagen type III and IV has been seen in the remodeled RV.³⁰ Here we found a significant reduction of collagen type IV alpha chains and collagen III alpha-1 chain in clodronate treated rats with SU-HX PH, suggesting RV macrophages may contribute to regulation of synthesis of these proteins.

We also found a significant reduction in collagen type I, fibrillary proteins and ECM glycoproteins in clodronate-treated rats, as well as reduction in other proteins important in the structural support of the ECM in functions of actin filament binding, actin cytoskeleton

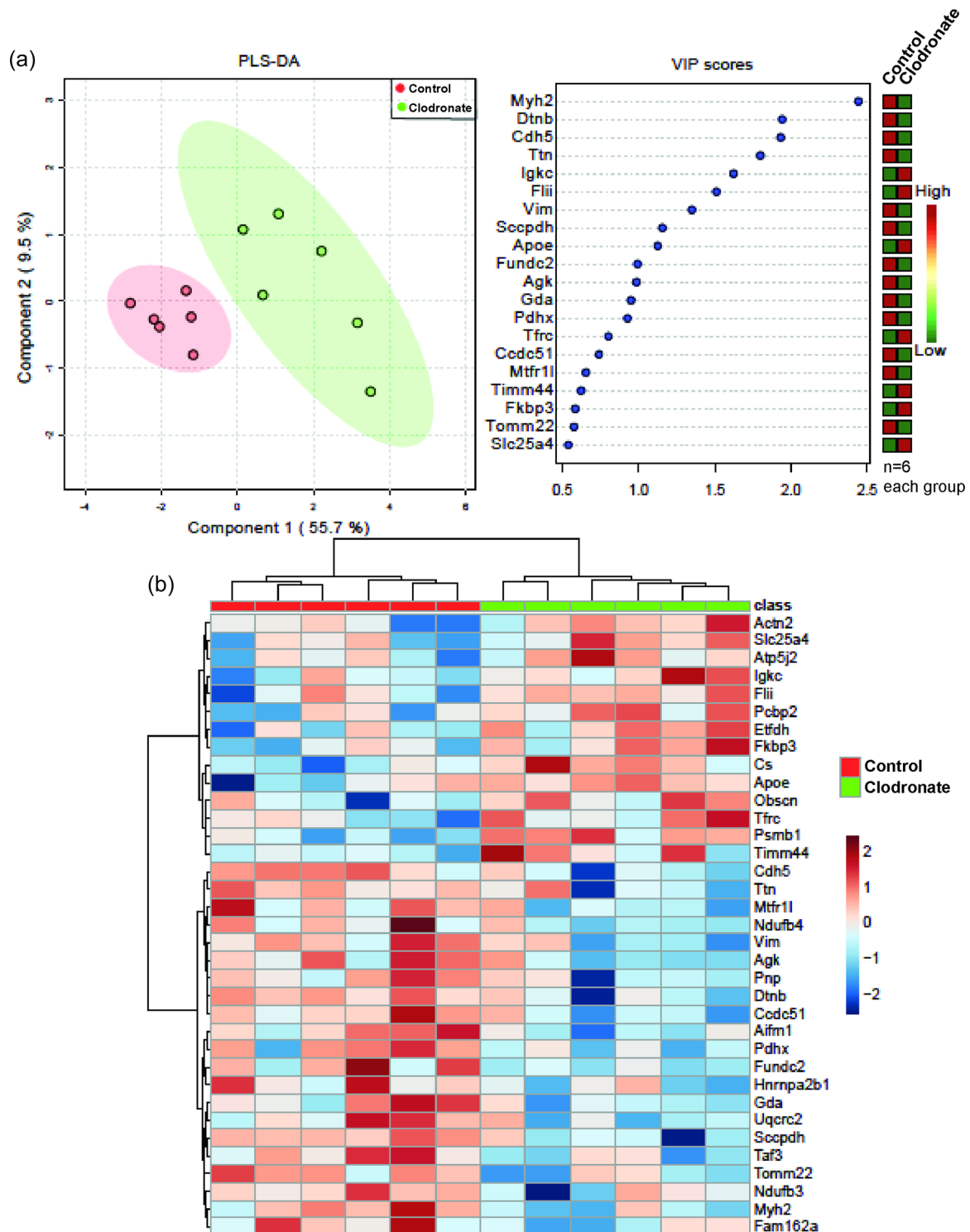


FIGURE 5 Clodronate treatment significantly alters nonextracellular matrix (ECM) proteins in Rat Sugen hypoxia (SU-HX) (a). Principal component analysis of non-ECM proteins in SU-HX rats that received PBS liposomes (control) compared to clodronate liposomes (drug) (b). Heat map with expression of non-ECM proteins in control compared to clodronate treated SU-HX rats with differentially expressed proteins with $p \leq 0.05$. PBS, phosphate buffered saline; PLS-DA, partial least squares-discriminant analysis; VIP, variable importance projection.

organization, cell adhesion, and muscle assembly. There were also decreases in mitochondrial functions, purine metabolism and salvage, and an increase in lipid metabolism along with upregulation of APOE, a protein

with pleomorphic effects in cardiovascular disease and mortality. The role of nonstructural ECM and non-ECM proteins in RV remodeling is not yet understood, but our findings highlight the need to further study these

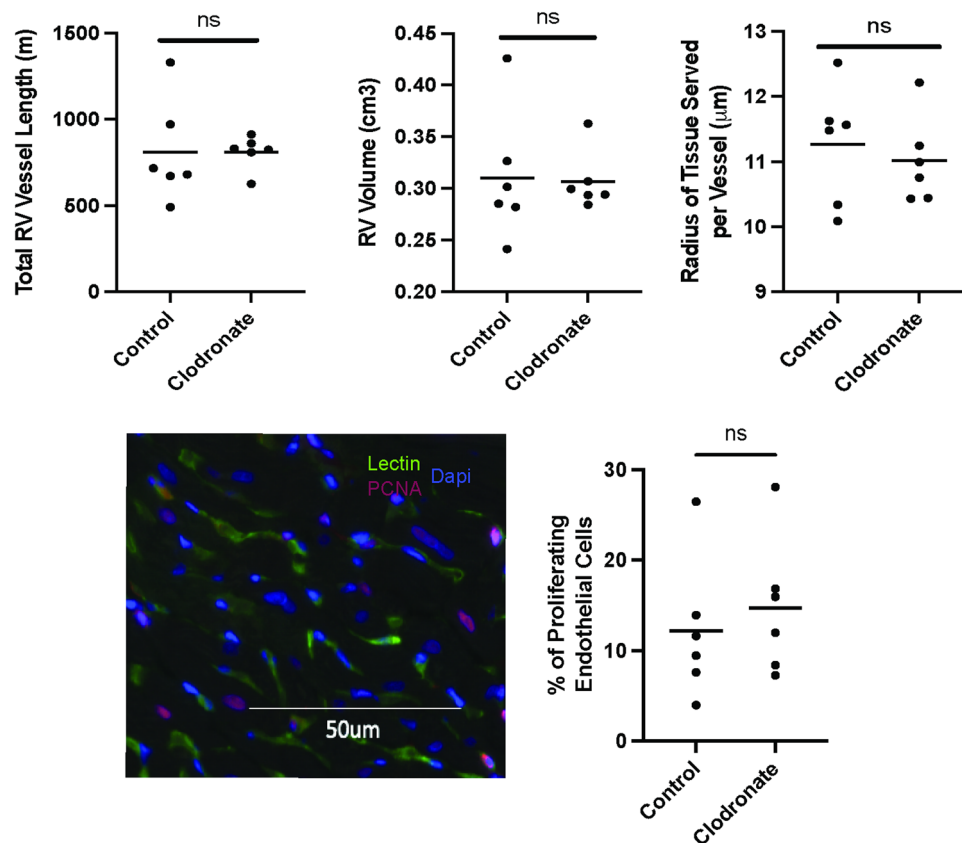


FIGURE 6 Clodronate treatment does not affect right ventricular (RV) vascular adaptation in pulmonary hypertension (PH). Total RV vascular length, RV free wall volume, and radius of tissue served per vessel in PBS liposome treated (control) and clodronate treated Sugen hypoxia rats ($n = 6$ per group, t -test, ns). RV volume, RV vessel length, and percentage of proliferating endothelial cells determined from rat RV tissue stained for lectin (green), proliferating cell nuclear antigen (PCNA, red), and dapi (blue). Percent of proliferating endothelial cells were triple positive for lectin + PCNA + dapi and divided by lectin + dapi double positive cells. ns, nonsignificant.

processes. These ECM and non-ECM protein changes were associated with functional improvements in RV contractility and RV/PA coupling in our study, and our findings could indicate that macrophages play a role in RV remodeling. These are supported by conclusions of another study on experimental PH in rats using PA banding, in which inhibition of TLR9-NF- κ B pathway-mediated sterile inflammation was associated with decreased macrophage infiltration and concomitant decreased fibrosis in the right ventricle.³¹

Our findings of stable total macrophage numbers are consistent with the finding that total CD68 cardiac macrophages were not increased in one autopsy series of human RV tissue in the setting of chronic idiopathic pulmonary arterial hypertension (IPAH).³² This contrasts with the finding of increased RV macrophages in the same autopsy series on patients that died from acute pulmonary embolism,³³ another investigation showing increased RV macrophages in patients with systemic sclerosis-associated PH compared to IPAH,³⁴ and a third study comprised mostly of IPAH patients but that also

included PH and chronic thromboembolic pulmonary hypertension which reported increased RV macrophages.³⁵ In an experiment using the VEGFR2 inhibitor sumatinib to induce PH in rats, increased RV CD68 macrophages were seen and were correlated with RV dilation and decreased fractional area change.³⁶ A limitation of these previous studies is their observational nature, which did not establish a clear relationship between RV macrophages and RV function, and that they did not attempt to quantify subsets of macrophages. However, in aggregate they suggest that macrophage expansion in the RV increases with greater acuity of RV pressure overload, and potentially in specific etiologies of PH, and thus our experimental findings must be carefully interpreted within these contexts.

The presence of at least three macrophage subpopulations in tissues including the lung and adult heart at steady state gated based on surface markers CD11c and MHCII has been demonstrated previously.^{8,21} We observed an increase in two subsets of RV interstitial macrophages, IM1 (CD11c^{lo}MHCII^{lo}) and IM3 (CD11c^{hi}MHCII^{hi}),

following experimental PH challenge. Using parabiosis experiments, we found low levels of contribution to the cardiac macrophage population from circulating monocytes at steady state. Following two PH stimuli, acute hypoxia or schistosomiasis, there was no significant increase in circulating cell contribution to overall RV macrophages, while at least the IM3 (CD11c^{hi}MHCII^{hi}) subset had significantly increased circulation-derived cells in *Schistosomiasis*-PH. This is consistent with findings in the lung, in which transcriptional analysis of IM1 and IM3 subpopulations found high levels of inflammatory mediators and receptors as well as monocyte-related genes such as CD14, CD163, and Csf1, suggesting that these subpopulations may arise from circulating monocytes.²¹ Our findings are also consistent with recently published longer term parabiosis experiments showing that at steady state, MHCII^{hi} macrophages compared to other macrophage populations in the heart achieved higher degrees of chimerism from partner derived cells, although our gating strategy differs from these studies in that they additionally used markers LYVE1, TIMD4, FOLR2, and CCR2 to elucidate further macrophage subsets within the heart and other organs.³⁷ Other mechanisms of macrophage subtype expansion in experimental PH through changes in programming in response to signaling in the local tissue environment or by means of local proliferation have yet to be explored.

With regard to the limitations of these aforementioned parabiosis experiments, which use CD45.1 (B6.SJL-*Ptprca*^a*Pepcb*/Boy) mice due to presumption that this mouse strain is genetically identical to CD45.2 C57BL/6J mice other than at the CD45 locus, one study identified an additional point mutation in the natural cytotoxicity receptor 1 present on natural killer cells in CD45.1 mice that may increase susceptibility to certain viral infections.³⁸ While this finding is unlikely to have significance for the development of *Schistosoma*-PH, which we have previously characterized as a Th2 CD4⁺ T cell mediated type II inflammatory response,²² we acknowledge the possibility that CD45.1 and CD45.2 congenic mice may have differing immune responses.

While clodronate treatment is a well described method of depleting circulating monocytes/macrophages,³⁹ lung interstitial macrophages,⁴⁰ and resident cardiac macrophages,^{8,25–27} we observed a less clear effect on overall RV tissue macrophages at the time of assessment. Previous studies using clodronate depletion methods using a single IV injection of clodronate showed depletion of all resident cardiac macrophage populations by 4 days after clodronate treatment, but found that these populations begin to be repopulated at differing rates by Ly6C⁺ monocytes as well as through local proliferation of macrophages by Day 7,⁸ hence our choice to repeat

dosing of clodronate every 7 days. Our finding of a trend toward decreased tissue macrophages on Day 21, which was 7 days after the third and final clodronate treatment, may reflect a timepoint at which macrophages were repopulating the heart, affecting our ability to detect decreased RV macrophages. In spite of this, we postulate that modifications to the ECM as a result of macrophage depletion would remain, resulting in the persistent differences in the ECM and non-ECM proteins that we detected, as well as functional differences in RV contractility and RV/PA coupling.

While our study is one of the effects of macrophage depletion in a chronic, severe pressure overload state in which macrophages may be orchestrating a maladaptive response, other studies have demonstrated that macrophages may play an important role in early, acute cardiac injury. In a PA banding study, pretreatment with clodronate resulted in the death of a majority of the mice due to cardiac arrhythmias within days after PA banding, while mortality was not seen in antigranulocyte antibody treated mice or in CD4 or CD8 cell deficient transgenic mice.⁴⁰ Similarly, studies of experimental myocardial infarction (MI) have shown that early clodronate macrophage depletion resulted in increased infarct and scar size, LV dysfunction, and worse mortality, while late clodronate treatment after MI did not have these negative effects.^{25–27} These data support a paradigm in which macrophage subtypes that expand early after acute injury are necessary for survival, but either phenotypic changes or recruitment of other macrophage subtypes later in the course of injury may result in the presence of less beneficial or maladaptive responses. Future experiments utilizing more targeted macrophage depletion approaches and with a more specific timing of removal of macrophage populations early or late in the development of PH will be necessary to dissect this hypothesis more completely.

In conclusion, this is the first study of our knowledge to analyze macrophage heterogeneity in the RV at steady state and in response to experimental PH. We observed that RV macrophages likely contribute to RV remodeling through changes in the ECM, and that macrophage depletion with clodronate improved parameters of RV adaptation to experimental PH. We found diversity in the response of macrophage subtypes to experimental PH, with some populations recruited from the circulation while others may be derived from expansion of pre-existing interstitial cells. Future experiments will be needed to dissect mechanisms by which RV macrophages contribute to RV maladaptation, and further elucidate RV macrophage heterogeneity by understanding their origins and differences in programming at steady state and in PH.

AUTHOR CONTRIBUTIONS

The authors confirm contribution to the paper as follows. *Study conception and design:* Sue Gu, Brian B. Graham, Claudia Mickael, and Rubin M. Tuder. *Execution of experiments:* Sue Gu, Claudia Mickael, Rahul Kumar, Michael H. Lee, Linda Sanders, Biruk Kassa, Julie Harral, and Jason Williams. *Data analysis:* Sue Gu, Claudia Mickael, Michael H. Lee, Julie Harral, and Jason Williams. *Interpretation of results:* Sue Gu, Claudia Mickael, Jason Williams, Kirk C. Hansen, Kurt R. Stenmark, Rubin M. Tuder, and Brian B. Graham. *Primary draft manuscript preparation:* Sue Gu and Brian B. Graham. All authors reviewed the results and approved the final version of the manuscript.

ACKNOWLEDGMENTS

Schistosome-infected mice were provided by the NIAID Schistosomiasis Resource Center at the Biomedical Research Institute (Rockville, MD) through NIH-NIAID Contract HHSN27220100005I for distribution through BEI Resources. Grant funding was provided by the 2020 Entelligence Award (Actelion Pharmaceuticals) and PRIDE-AGOLD (NIH R25HL14166) (CM); American Heart Association Grant 19CDA34730030, Cardiovascular Medical Research and Education Fund (CMREF) and ATS Foundation/Pulmonary Hypertension Association Research Fellowship (RK); NIH Grant P01HL152961 (RMT and BBG); R01HL135872 (BBG), F32HL151076 (MHL), 5T32HL007085 (SG) and 5T32HL007171 (SG).

CONFLICT OF INTEREST

The authors declare no conflict of interest.

ETHICS STATEMENT

All animal experiments were approved by the University of Colorado Institutional Animal Care and Use Committee (Aurora, CO).

ORCID

Sue Gu  <http://orcid.org/0000-0002-2719-623X>

Michael H. Lee  <http://orcid.org/0000-0002-5739-8369>

Jason Williams  <http://orcid.org/0000-0002-8023-2607>

Brian B. Graham  <http://orcid.org/0000-0001-7541-2585>

REFERENCES

1. Benza RL, Miller DP, Barst RJ, Badesch DB, Frost AE, McGoon MD. An evaluation of long-term survival from time of diagnosis in pulmonary arterial hypertension from the REVEAL Registry. *Chest*. 2012;142:448–56.
2. D'Alonzo GE, Barst RJ, Ayres SM, Bergofsky EH, Brundage BH, Detre KM, Fishman AP, Goldring RM, Groves BM, Kernis JT. Survival in patients with primary pulmonary hypertension: results from a national prospective registry. *Ann Intern Med*. 1991 Sep 1;115:343–349.
3. Kalogeropoulos AP, Vega JD, Smith AL, Georgiopoulou VV. Pulmonary hypertension and right ventricular function in advanced heart failure. *Congestive Heart Failure*. 2011 Jul-Aug;17:189–98.
4. Lahm T, Douglas IS, Archer SL, Bogaard HJ, Chesler NC, Haddad F, Hemnes AR, Kawut SM, Kline JA, Kolb TM, Mathai SC, Mercier O, Michelakis ED, Naeije R, Tuder RM, Ventetuolo CE, Vieillard-Baron A, Voelkel NF, Vonk-Noordegraaf A, Hassoun PM, American Thoracic Society Assembly on Pulmonary Circulation. Assessment of right ventricular function in the research setting: knowledge gaps and pathways forward. An Official American Thoracic Society Research Statement. *Am J Respir Crit Care Med*. 2018 Aug 15;198:e15–43.
5. Graham BB, Kumar R, Mickael C, Kassa B, Koyanagi D, Sanders L, Zhang L, Perez M, Hernandez-Saavedra D, Valencia C, Dixon K, Harral J, Loomis Z, Irwin D, Nemkov T, D'Alessandro A, Stenmark KR, Tuder RM. Vascular adaptation of the right ventricle in experimental pulmonary hypertension. *Am J Respir Cell Mol Biol*. 2018 Oct;59:479–89.
6. Hulsmans M, Sam F, Nahrendorf M. Monocyte and macrophage contributions to cardiac remodeling. *J Mol Cell Cardiol*. 2016 Apr;93:149–55.
7. Ginhoux F, Greter M, Leboeuf M, Nandi S, See P, Gokhan S, Mehler MF, Conway SJ, Ng LG, Stanley ER, Samokhvalov IM, Merad M. Fate mapping analysis reveals that adult microglia derive from primitive macrophages. *Science*. 2010;330:841–845.
8. Epelman S, Lavine KJ, Beaudin AE, Sojka DK, Carrero JA, Calderon B, Brijja T, Gautier EL, Ivanov S, Satpathy AT, Schilling JD, Schwendener R, Sergin I, Razani B, Forsberg EC, Yokoyama WM, Unanue ER, Colonna M, Randolph GJ, Mann DL. Embryonic and adult-derived resident cardiac macrophages are maintained through distinct mechanisms at steady state and during inflammation. *Immunity*. 2014 Jan 16;40:91–104.
9. Svedberg FR, Williams M. Cellular origin of human cardiac macrophage populations. *Nat Med*. 2018 Aug;24:1–2.
10. Bajpai G, Schneider C, Wong N, Bredemeyer A, Hulsmans M, Nahrendorf M, Epelman S, Kreisel D, Liu Y, Itoh A, Shankar TS, Selzman CH, Drakos SG, Lavine KJ. The human heart contains distinct macrophage subsets with divergent origins and functions. *Nat Med*. 2018 Aug;24:1234–45.
11. Patel B, Bansal SS, Ismahil MA, Hamid T, Rokosh G, Mack M, Prabhu SD. CCR2+ monocyte-derived infiltrating macrophages are required for adverse cardiac remodeling during pressure overload. *JACC Basic Transl Sci*. 2018 Apr;3:230–44.
12. Westermann D, Lindner D, Kasner M, Zietsch C, Savvatis K, Escher F, von Schlippenbach J, Skurk C, Steendijk P, Riad A, Poller W, Schultheiss HP, Tschöpe C. Cardiac inflammation contributes to changes in the extracellular matrix in patients with heart failure and normal ejection fraction. *Circ Heart Fail*. 2011 Jan;4:44–52.
13. Kagitani S, Ueno H, Hirade S, Takahashi T, Takata M, Inoue H. Tranilast attenuates myocardial fibrosis in association with suppression of monocyte/macrophage infiltration in

- DOCA/salt hypertensive rats. *J Hypertens*. 2004 May;22:1007–15.
14. Nucera S, Biziato D, De Palma M. The interplay between macrophages and angiogenesis in development, tissue injury and regeneration. *Int J Dev Biol*. 2011;55:495–503.
 15. Garg K, Sell SA, Madurantakam P, Bowlin GL. Angiogenic potential of human macrophages on electrospun bioresorbable vascular grafts. *Biomed Mater*. 2009;4:031001–10.
 16. Graham BB, Mentink-Kane MM, El-Haddad H, Purnell S, Zhang L, Zaiman A, Redente EF, Riches DW, Hassoun PM, Bandeira A, Champion HC, Butrous G, Wynn TA, Tudor RM. Schistosomiasis-induced experimental pulmonary hypertension. *Am J Pathol*. 2010 Sep;177:1549–61.
 17. Taraseviciene-Stewart L, Kasahara Y, Alger L, Hirth P, Mc Mahon G, Waltenberger J, Voelkel NF, Tudor RM. Inhibition of the VEGF receptor 2 combined with chronic hypoxia causes cell death-dependent pulmonary endothelial cell proliferation and severe pulmonary hypertension. *FASEB J*. 2001 Feb;15:427–38.
 18. Kamran P, Sereti K-I, Zhao P, Ali SR, Weissman IL, Ardehali R. Parabiosis in mice: a detailed protocol. *JoVE*. 2013 Oct 6;80:e50556.
 19. Tschanz SA, Burri PH, Weibel ER. A simple tool for stereological assessment of digital images: the STEPanizer. *J Microsc*. 2011 Jul;243:47–59.
 20. Gautier EL, Shay T, Miller J, Greter M, Jakubzick C, Ivanov S, Helft J, Chow A, Elpek KG, Gordonov S, Mazloom AR, Ma'ayan A, Chua WJ, Hansen TH, Turley SJ, Merad M, Randolph GJ, Immunological Genome Consortium. Gene-expression profiles and transcriptional regulatory pathways that underlie the identity and diversity of mouse tissue macrophages. *Nat Immunol*. 2012 Nov;13:1118–28.
 21. Gibbings SL, Thomas SM, Atif SM, McCubbrey AL, Desch AN, Danhorn T, Leach SM, Bratton DL, Henson PM, Janssen WJ, Jakubzick CV. Three unique interstitial macrophages in the murine lung at steady state. *Am J Respir Cell Mol Biol*. 2017 Jul;57:66–76.
 22. Kumar R, Mickael C, Kassa B, Sanders L, Koyanagi D, Hernandez-Saavedra D, Freeman S, Morales-Cano D, Cogolludo A, McKee AS, Fontenot AP, Butrous G, Tudor RM, Graham BB. Th2 CD4+ T cells are necessary and sufficient for Schistosoma-pulmonary hypertension. *J Am Heart Assoc*. 2019 Aug 6;8:e013111.
 23. Frid MG, Brunetti JA, Burke DL, Carpenter TC, Davie NJ, Reeves JT, Roedersheimer MT, van Rooijen N, Stenmark KR. Hypoxia-induced pulmonary vascular remodeling requires recruitment of circulating mesenchymal precursors of a monocyte/macrophage lineage. *Am J Pathol*. 2006 Feb;168:659–69.
 24. Bowers SLK, Banerjee I, Baudino TA. The extracellular matrix: at the center of it all. *J Mol Cell Cardiol*. 2010 Mar;48:474–82.
 25. van Amerongen MJ, Harmsen MC, van Rooijen N, Petersen AH, van Luyn MJA. Macrophage depletion impairs wound healing and increases left ventricular remodeling after myocardial injury in mice. *Am J Pathol*. 2007;170:818–29.
 26. Nahrendorf M, Swirski FK, Aikawa E, Stangenberg L, Wurdinger T, Figueiredo JL, Libby P, Weissleder R, Pittet MJ. The healing myocardium sequentially mobilizes two monocyte subsets with divergent and complementary functions. *J Exp Med*. 2007;204:3037–47.
 27. Ben-Mordechai T, Holbova R, Landa-Rouben N, Harel-Adar T, Feinberg MS, Abd Elrahman I, Blum G, Epstein FH, Silman Z, Cohen S, Leor J. Macrophage subpopulations are essential for infarct repair with and without stem cell therapy. *J Am Coll Cardiol*. 2013 Nov 12;62:1890–1901.
 28. Ambade AS, Hassoun PM, Damico RL. Basement membrane extracellular matrix proteins in pulmonary vascular and right ventricular remodeling in pulmonary hypertension. *Am J Respir Cell Mol Biol*. 2021 Sep;65:245–58.
 29. Pöschl E, Schlötzer-Schrehardt U, Brachvogel B, Saito K, Ninomiya Y, Mayer U. Collagen IV is essential for basement membrane stability but dispensable for initiation of its assembly during early development. *Development*. 2004 Apr;131:1619–28.
 30. Perhonen M, Wang W, Han X, Ruskoaho H, Takala TE. Right ventricular collagen type III and IV gene expression increases during early phases of endurance training in hypobaric hypoxic condition. *Basic Res Cardiol*. 1997 Oct;92:299–309.
 31. Yoshida K, Abe K, Saku K, Sunagawa K. Inhibition of Nuclear Factor-kappaB-Mediated Inflammation Reverses Fibrosis and Improves RV Function in Rats with Pulmonary Artery Banding. *J Card Failure*. 2016;22:S198.
 32. Begieneman MP, van de Goot FR, van der Bilt IA, Vonk Noordegraaf A, Spreeuwenberg MD, Paulus WJ, van Hinsbergh VW, Visser FC, Niessen HW. Pulmonary embolism causes endomyocarditis in the human heart. *Heart*. 2008 Apr;94:450–456.
 33. Iwadate K, Doi M, Tanno K, Katsumura S, Ito H, Sato K, Yonemura I, Ito Y. Right ventricular damage due to pulmonary embolism: examination of the number of infiltrating macrophages. *Forensic Sci Int*. 2003 Jul 8;134:147–53.
 34. Overbeek MJ, Mouchaers KTB, Niessen HM, Hadi AM, Kupreishvili K, Boonstra A, Voskuyl AE, Belien JAM, Smit EF, Dijkman BC, Vonk-Noordegraaf A, Grünberg K. Characteristics of interstitial fibrosis and inflammatory cell infiltration in right ventricles of systemic sclerosis-associated pulmonary arterial hypertension. *Int J Rheumatol*. 2010;2010:1–10.
 35. Nergui S, Fukumoto Y, Doe Z, Nakajima S, Shimizu T, Ikeda S, Elias-Al-Mamun M, Shimokawa H. Role of endothelial nitric oxide synthase and collagen metabolism in right ventricular remodeling due to pulmonary hypertension. *Circ J*. 2014;78:1465–74.
 36. Guihaire J, Deuse T, Wang D, Fadel E, Reichenspurner H, Robbins RC, Schrepfer S. Pulmonary hypertension macrophage infiltration correlates with right ventricular remodeling in an experimental model of pulmonary hypertension. *J Heart Lung Transplant*. 2017;36:S370–71.
 37. Dick SA, Wong A, Hamidzada H, Nejat S, Nechanitzky R, Vohra S, Mueller B, Zaman R, Kantores C, Aronoff L, Momen A, Nechanitzky D, Li WY, Ramachandran P, Crome SQ, Becher B, Cybulsky MI, Billia F, Keshavjee S, Mital S, Robbins CS, Mak TW, Epelman S. Three tissue resident macrophage subsets coexist across organs with conserved origins and life cycles. *Sci Immunol*. 2022 Jan 7;7:eabf7777.

38. Jang Y, Gerbec ZJ, Won T, Choi B, Podsiad A, B Moore B, Malarkannan S, Laouar Y. Cutting edge: check your mice-A point mutation in the Ncr1 locus identified in CD45.1 congenic mice with consequences in mouse susceptibility to infection. *J Immunol*. 2018 Mar 15;200:1982–87.
39. van Rooijen N, Sanders A. Liposome mediated depletion of macrophages: mechanism of action, preparation of liposomes and applications. *J Immunol Methods*. 1994 Sep 14;174:83–93.
40. Sugita J, Fujii K, Nakayama Y, Matsubara T, Matsuda J, Oshima T, Liu Y, Maru Y, Hasumi E, Kojima T, Seno H, Asano K, Ishijima A, Tomii N, Yamazaki M, Kudo F, Sakuma I, Nagai R, Manabe I, Komuro I. Cardiac macrophages prevent sudden death during heart stress. *Nat Commun*. 2021 Mar 26;12:1–10.

SUPPORTING INFORMATION

Additional supporting information can be found online in the Supporting Information section at the end of this article.

How to cite this article: Gu S, Mickael C, Kumar R, Lee MH, Sanders L, Kassa B, Harral J, Williams J, Hansen KC, Stenmark KR, Tudor RM, Graham BB. The role of macrophages in right ventricular remodeling in experimental pulmonary hypertension. *Pulmonary Circulation*. 2022;12:e12105. <https://doi.org/10.1002/pul2.12105>